# 学位申請論文

井口正人

# A Vertical Expansion Source Model for the Mechanisms of Earthquakes Originated in the Magma Conduit of an Andesitic Volcano: Sakurajima, Japan

Masato Iguchi

*Sakurajima Volcanological Observatory, Disaster Prevention Research Institute, Kyoto University, Sakurajima, Kagoshima 891-14, Japan*

主論文

# A Vertical Expansion Source Model for the Mechanisms of Earthquakes Originated in the Magma Conduit of an Andesitic Volcano: Sakurajima, Japan

Masato Iguchi

*Sakurajima Volcanological Observatory, Disaster Prevention Research Institute, Kyoto University, Sakurajima, Kagoshima 891-14, Japan*

## Contents

## Abstract

Volcanic earthquakes associated with the activity of summit eruptions at Sakurajima, an andesitic volcano in Japan, are classified into four groups: "A-type", "BH-type", "BL-type" and "explosion" earthquakes. These earthquakes are originated in a vertically elongated zone at depths from 1 to 4 km beneath the summit crater. Source mechanisms of these earthquakes are investigated by application of the inversion for a second derivative of moment tensor using amplitudes of the first motions of P-waves. Double-couple components are dominant in A-type earthquakes as in tectonic ones. Considering the fact that high-frequency components greater than 10 Hz are dominant and that the hypocenters are distributed around the conduit, A-type earthquakes are inferred to be generated by shear faulting in brittle rocks surrounding the conduit. In contrast to this, non-double-couple components, especially vertical dipoles, are dominant in BH-type, BL-type and explosion earthquakes. The result is supported by the dominance of SV-waves. These three types of earthquakes are lacking in high-frequency components and their hypocenters are located within the conduit. The vertical dipole may be associated with expansion process of gas pocket in the conduit.

The difference in dominant frequencies among BH-type, BL-type and explosion earthquakes may be attributed to their source processes. A possible interpretation of the difference is that source processes of these earthquakes are different depending on the state of the magma conduit.

## 1. Introduction

Earthquakes and tremors with a variety of waveforms have been observed at active volcanoes. Minakami (1974) proposed a classification of volcanic earthquakes into "A-type", "B-type" and "explosion" earthquakes based on observations at Asama, Sakurajima and other volcanoes in Japan. A-type earthquakes have distinct P and S phases similar to those of shallow tectonic earthquakes and occur at depths from 1 to 20 km. B-type and explosion earthquakes have different characteristics. B-type earthquakes originate at a shallower level less than 1 km, and their S-phases in the seismograms are not clear and the periods of vibration range from 0.2 to 1.0 second. Explosion earthquakes are related to violent eruptions with rapid ejection of volcanic materials.

Recent precise determinations of hypocenters have revealed that the focal depths of B-type earthquakes extend to 3 km. The hypocentral depths are inconsistent with the depth required by the Minakami's criteria for B-type earthquakes. Therefore, some volcanologists have proposed new classifications of volcanic earthquakes based on their hypocentral locations or spectra, for examples, those at Ruapehu and Ngauruhoe volcanoes by Latter (1981) and those at St. Helens by Endo *et al.* (1981) and Malone (1983).

Nevertheless, the Minakami's classification has been applied successfully to volcanic earthquakes at several andesitic volcanoes with minor modification, for examples, at Pavlof by McNutt (1986), at Suwanosejima by Iguchi (1991) and at Arenal by Barquero *et al.* (1992). A-type earthquakes have often preceded the

swarms of B-type ones, and the swarms have been followed by explosive activity (Kamo, 1978). This may be one of the reasons why the Minakami's classification has been used. More detailed classifications for B-type earthquakes have been proposed at Sakurajima and Asama volcanoes to make clear the relationship of B-type earthquakes to the following explosive eruptions (Yoshikawa and Nishi, 1965; Shimozuru and Kagiyama, 1989). Recently, Ishihara and Iguchi (1989) classified B-type earthquakes into high (BH) and low frequency (BL) types and showed that their respective volcanic processes are different.

The source mechanisms of A-type and explosion earthquakes have been studied at Sakurajima and Asama volcanoes by means of spatial distribution of the first motions of P-wave. The push-pull pattern of A-type earthquakes is of the quadrant type similar to tectonic ones (Minakami, 1974; Nishi, 1978). By contrast, the first motions of explosion earthquakes are compressions at all stations (Minakami, 1974; Yamasato, 1987). A model of isotropic expansion has been applied to estimation of source parameters for explosion earthquakes by Nishi (1980) and Imai (1980).

The source mechanism of B-type earthquakes has been scarcely studied because of their emergent onset. In order to clearly detect the first motions of B-type earthquakes, borehole seismometers were installed around the summit crater of Sakurajima Volcano. Using records obtained by the borehole seismometers, Iguchi (1989) clarified the difference in focal depths between BH-type and BL-type and showed that the polarities of the first motions were the same at all stations.

Previous researchers have studied the source mechanism for each type of volcanic earthquake only individually. In the present study, volcanic earthquakes at

Sakurajima Volcano are classified into four types: A-type, BH-type, BL-type and explosion earthquakes, and they were analyzed together in a similar manner as described below.

First, their fundamental features of every type of earthquakes were clarified by examining spectrum, hypocenter, polarity of P-waves and polarization direction of S-waves. Next, source mechanisms were described by a second derivative of moment tensor, which was estimated by an inversion from the amplitudes of P-waves at several seismic stations. Finally, the source mechanisms of every type were mutually compared and are discussed in relation to the structure and state of the magma conduit.

## 2. Observations

Sakurajima Volcano is an andesitic stratovolcano located in South Kyushu, Japan (Fig. 1). Eruptive activity has continued since 1955 at the summit crater of the central cone, "Minamidake", and three styles of eruptive activity are manifested, namely, Vulcanian explosion, non-explosive eruption and continuous eruption (Kamo and Ishihara, 1989).

The locations of seismic stations employed in the present study are shown in Fig. 1. Eight stations are distributed around the active crater with distances from the crater ranging from 1.7 to 4.5 km. Borehole seismometers of 3-components are operated at four stations and ground-based ones are installed at four other stations. The specifications of the seismometers are described in Table 1. Seismic signals from each station have been transmitted to Sakurajima Volcanological Observatory (SVO) via telephone lines or radio waves. The seismic signals have

been recorded at the observatory on analog magnetic tapes by an event trigger system.

## 3. Features of volcanic earthquakes

In this chapter, the spectra, hypocenters, polarities of P-waves and polarizations of S-waves are described for A-type, BH-type, BL-type and explosion earthquakes.

Typical seismograms of the four types of volcanic earthquakes obtained by borehole seismometers are shown in Fig. 2. A-type earthquakes have clear P and S phases and high-frequency components. The ratio of the maximum amplitude of P-waves to that of S-waves differs depending on stations as expected from the quadrant-type source mechanism. In seismograms of BH-type, BL-type and explosion earthquakes, lower-frequency components are dominant, and it is difficult to identify S-phases. An apparent waveform of BL-type earthquakes is similar to that of explosion earthquakes, but some characteristics are different, however, which will be discussed later.

For A-type, BH-type, BL-type and explosion earthquakes, the waveforms are similar to each other between the four stations. This suggests that the difference in waveforms may neither be attributed to the propagation path nor to the site effect but to the source effect.

### 3-1 Spectrum

In order to better distinguish and identify the waveforms of the four types of volcanic earthquakes, velocity spectra were examined. Fast Fourier Transform was

applied to the waveforms digitized at the rate of 100 samples per second. The time window of the FFT analysis is 10.24 seconds from the onset of the first motions. No instrumental correction was made. The spectra of 66 earthquakes were calculated. A-type, BH-type and explosion earthquakes have similar spectral patterns, respectively. The typical spectra of these earthquakes are plotted in logarithmic scales as shown in Fig. 3(a), (b) and (d). BL-type earthquakes have variety in spectrum, and two typical spectra are shown in Fig. 3(c)

In A-type earthquakes, frequency contents of 10 to 20 Hz are dominant. By contrast, seismograms of BH-type, BL-type and explosion earthquakes are commonly lacking in the frequency contents higher than 10 Hz.

BH-type, BL-type and explosion earthquakes have dominant peaks at 5～8 Hz, 1～3 Hz and 0.5～3 Hz, respectively. Dominant frequencies of BL-type earthquakes which occur in isolation are about 1 Hz as shown by a solid line in Fig. 3(c), and those in swarms have higher-frequency peaks at about 3 Hz as shown by a broken line (Iguchi, 1989). The range of dominant frequency of BL-type is not clearly discriminated from that of explosion earthquakes as expected from the similarity of their waveforms. However, two significant differences are recognized in Fig. 3. One is that explosion earthquakes have larger amplitudes than BL-type ones do. The other is that BL-type earthquakes have relatively narrow prominent peaks, whereas explosion earthquakes have a wider width in predominant frequencies. It is noted that in the spectra of explosion earthquakes, the amplitudes with frequency of 0.5 to 2.0 Hz are almost constant with the perturbation of 4 dB.

### 3-2 Hypocentral location

The hypocenters of A-type and explosion earthquakes at Sakurajima Volcano have been determined by the routine job of Sakurajima Volcanological Observatory (Kamo, 1978; Ishihara, 1990). Here, the hypocenters of BH-type and BL-type earthquakes were determined from the onset times of P-wave at eight stations, assuming a homogeneous medium of $V_p$=2.5 km/s. The number of stations employed for the determination of hypocenters was fixed to eight in order to minimize the errors associated with the combination of the stations. Because each station has a peculiar residual time with a fluctuation of ±0.03 second, the station correction values were determined by averaging the residual times. After correction of arrival times, standard errors in the determination of hypocenters were reduced to less than 0.15 and 0.5 km in horizontal and vertical planes, respectively. Hypocentral locations of BH-type and BL-type earthquakes are illustrated in Fig. 4 with a focal zone of explosion earthquakes and the locations of A-type earthquakes determined in this as well as in previous studies (Kamo, 1978; Ishihara, 1990).

The hypocenters of explosion earthquakes are concentrated in a cylindrical zone with a radius of about 200 m at depths from 1 to 3 km beneath the summit crater (Fig. 4). On the other hand, A-type earthquakes are distributed around the zone at depths from 1 to 4 km. The cylindrical zone is believed to correspond to the magma conduit (Ishihara, 1990). Because most of BH-type and BL-type earthquakes are located in the cylindrical zone, it is inferred that BH-type and BL-type earthquakes also occur in the magma conduit as do explosion earthquakes.

The ranges of hypocentral depths are different between the BL-type and BH-

type earthquakes. The BL-type earthquakes are originated at depths of less than 3 km beneath the crater bottom. The hypocentral zone of BH-type earthquakes extends slightly deeper (2 to 3.5 km) than that of BL-type earthquakes. It is noteworthy that BH-type, BL-type and explosion earthquakes coexist in the range of common depths from 2 to 3 km.

### 3-3 Polarity of P-waves

Analysis of the distribution of the first motion of P-wave is a fundamental step to determine the source mechanism of earthquakes. Distributions of the polarities of the first motions generated by A-type, BH-type, BL-type and explosion earthquakes are plotted on maps of an equal-area projection on the upper hemisphere (Fig. 5).

The push-pull pattern of A-type earthquakes is of the quadrant type as indicated by Minakami (1974) and Nishi (1978) and is similar to that of tectonic ones which have double-couple source mechanism.

By contrast, the polarities of BH-type, BL-type and explosion earthquakes are the same at all stations. They are different from the tectonic ones. The first motions of BH-type and explosion earthquakes are "up" in the vertical components and "push" in the radial ones. Most of BL-type earthquakes which occur in isolation, have also compressional arrivals at all stations.

However, when BL-type earthquakes occur in swarms, they indicate a somewhat complicated manner. Iguchi (1989) examined 110 BL-type earthquakes in swarms and found 67 earthquakes of compressional arrivals and 39 of dilatational ones. The first motions of the 4 remainders appeared to be a mixture of compressions

and dilatations. These first motions were misidentified because errors associated with hypocentral determinations were 2 to 4 times greater than those of BL-type earthquakes with all compressional arrivals.

The distributions of the first motions of P-waves suggest that the source mechanisms of BH-type, BL-type and explosion earthquakes are not double couple.

### 3-4 Polarization of S-waves

It is expected that polarization directions of S-waves would give an additional constraint for the modelling of source mechanism. The polarization directions of S-waves were examined using particle motion diagrams and seismograms processed by applying a polarization filter (Montalbetti and Kanasewich, 1970; Iguchi, 1985).

Particle motions of A-type, BH-type, BL-type and explosion earthquakes observed at station HAR are plotted on a horizontal plane and on a vertical cross-section in the direction to the crater as shown in Fig. 6, where the particle motions of the four types are shown in three time windows, respectively. The arrival time of S-wave of A-type earthquake is discriminated 1.0 second after the onset time of P-wave. S-waves of BH-type, BL-type and explosion earthquakes are expected to arrive 0.7~0.9 second after the onset of P-waves from the focal distances, as indicated by "Sest" in Fig. 6(b)~(d). Particle motions of BH-type, BL-type and explosion earthquakes began to be polarized to the directions perpendicular to wave propagation 0.8, 1.0 and 0.9 second after the onset of P-waves, respectively, as shown by "Sx" in the second time windows of the same

figures. The arrival times of "Sx" phases almost coincide with those of the estimated arrival times of S-waves "Sest". This suggests that "Sx" phases are caused by S-waves.

The polarization directions of S-waves of BH-type, BL-type and explosion earthquakes are different from that of A-type earthquakes. The S-wave of A-type earthquakes appears in both vertical (SV-wave) and horizontal (SH-wave) components at the same time as shown in the third time window of Fig. 6(a). On the other hand, the particle motions of S-waves of BH-type, BL-type and explosion earthquakes are polarized in the vertical plane of wave propagation as shown in the second time windows of Fig. 6(b)~(d). Transverse components in the horizontal planes are smaller than longitudinal ones in the second time windows but become significant 1~2 seconds later as shown in the third ones of Fig. 6(b)~(d).

To enhance the polarization direction of S-waves, the waveforms are processed by applying the polarization filter (Fig. 7). The vertical (V) and longitudinal (L) components are rotated to the direction of seismic wave propagation, "Lon." and that perpendicular to it, "Per.", respectively, as shown in Fig. 7(e). The traces of "Lon.", "Per." and "Tran." correspond to motions of P-wave, SV-wave and SH-wave, respectively. SV- and SH-waves of A-type earthquakes appear at the same time. In the processed seismograms of BH-type, BL-type and explosion earthquakes, significant SV-waves are found at the expected arrival times of S-wave, and SH-wave components appear a few seconds later. The dominance of SV-waves are commonly recognized in every record obtained by borehole seismometers. This is a strong constraint on the source mechanism of BH-type,

BL-type and explosion earthquakes as well as the polarity of P-wave.

## 4. Estimation of second derivative of moment tensor

The radiation pattern of P-wave is the most useful information to determine the source mechanisms of BH-type, BL-type and explosion earthquakes. However, the amplitude of earthquakes is strongly affected by geological condition at each seismic station depending on whether seismometers are installed on lava or pumice layers (Minakami, 1970). At first, site effect around the stations was evaluated for the correction of the amplitude of the first motions, and distribution of amplitudes of P-waves was investigated using seismograms of 3-components. Next, a second derivative of moment tensor was estimated from the amplitude distribution.

### 4-1 Amplitude distribution of P-waves

In order to evaluate the site effect around the stations, first motions of P-wave of teleseismic events propagating from different azimuths were used on the assumption that the amplitudes of the teleseismic events should be the same at all stations in Sakurajima. The factor of site effect at each station was determined by averaging the ratio of amplitude at the station to that at station KOI, where the largest first motions were observed among the stations. Amplitude data of seismic waves propagating beneath the summit crater were ignored because they are strongly attenuated due to the magma reservoir (Ishihara, 1990). The averaged amplitude ratios and their standard deviations at borehole stations ARI, HAR, KAB and KOM are 0.39±0.17, 0.22±0.06, 0.22±0.08 and 0.23±0.10, respectively, and those at ground-based stations HIK, FUR, GON and NOJ are 0.59±0.14, 0.54±0.25,

0.93±0.39 and 0.68±0.19, respectively. The averaged ratios at the ground-based stations are a few times larger than those at borehole stations. The difference is attributed to the effect of free surface and partly to that of unconsolidated layer under the ground-based stations. The correction factors are defined as reciprocals of the averaged ratios of amplitude as listed in the first line of Table 2.

The corrected amplitudes for each type of earthquake are also listed in Table 2 and are plotted on the maps of an equal-area projection on the upper hemisphere (Fig. 8). The amplitude distribution of the A-type earthquake depends on both azimuth and distance as expected from the source mechanism of strike-slip fault type determined by the push-pull pattern. In contrast to this, the amplitude distributions of BH-type, BL-type and explosion earthquakes are independent of the azimuth from the hypocenters. The amplitudes are the maximum at the nearest station to the hypocenter and decrease smoothly with focal distances.

The BH-type earthquake is more strongly attenuated than the BL-type and explosion earthquakes due to inelastic attenuation. This was taken into account in amplitude inversion as described in the following section.

### 4-2 Amplitude Inversion of P-waves

The components of a second derivative of moment tensor for A-type, BH-type, BL-type and explosion earthquakes were estimated using the distribution of velocity amplitude of the first motion of P-waves taking inelastic attenuation and geometric spreading into consideration.

Displacement of P-waves $u^P$ generated from a point source with general moment tensor at the far-field is given by Aki and Richards (1980) as follows:

$$\mathbf{u}^P(\mathbf{x},t) = \left( \frac{\gamma \cdot \dot{\mathbf{M}}(t - \frac{r}{V_P}) \cdot \gamma}{4\pi\rho V_P{}^3 r} \right) \mathbf{l}, \tag{1}$$

where

ρ density,

$V_p$ propagation velocity of P-wave,

$r$ distance,

$t$ time,

**l** direction of wave propagation,

γ departing direction at the source, and

**M** moment tensor.

As only amplitudes of the first motions are treated here, the phase term is neglected. Inelastic attenuation $Q_p$ is taken into account, assuming that $Q_p$ is independent of frequency. Then, the amplitude of particle velocity is obtained as follows:

$$\dot{u}^P(\mathbf{x}) = \frac{F_P(\theta, \xi) \exp\left( -\frac{\omega r}{2V_P Q_P} \right)}{4\pi\rho V_P{}^3 r}, \tag{2}$$

where ω, θ and ξ are the angular frequency, azimuth from the source to seismic station and take-off angle of seismic wave from the source, respectively, and the coordinates system in the present analysis is shown in Fig. 9. $F_p(\theta, \xi)$ is a function which represents radiation pattern and is written as

$$F_p(\theta,\xi) = (\ddot{M}_{xx}\cos^2\theta + \ddot{M}_{yy}\sin^2\theta)\sin^2\xi + \ddot{M}_{zz}\cos^2\xi + 2\ddot{M}_{xy}\sin^2\xi\sin\theta\cos\theta + 2(\ddot{M}_{xz}\cos\theta + \ddot{M}_{yz}\sin\theta)\sin\xi\cos\xi, \quad (3)$$

and $M_{ij}$ is a Cartesian component of a moment tensor. The velocity amplitude is a linear combination of six components of a second derivative of moment tensor. The components were obtained by applying the least-squares method using amplitudes at all stations. In the calculation, a homogeneous medium of $V_p$=2.5 km/s was assumed, and the ray path from the source to seismic station was treated as straight line. $Q_p$ value was estimated to be 20 by comparing theoretical amplitude distribution with observed one in A-type earthquakes whose source mechanisms were definitely determined by the push-pull patterns of the first motions of P-wave. This $Q_p$ is comparable to the $Q$-factors of 25 and 45 at volcanoes (McNutt, 1986) and 50~100 in caldera areas (Sudo, 1991).

The estimated components of second derivative of moment tensor for A-type, BH-type, BL-type and explosion earthquakes are summarized in Table 3. Examples for the four types of seismic events are shown in Fig. 10. For the A-type earthquake, one of the double-couple components ($\ddot{M}_{xy}$) is the maximum. The dominance of the double-couple component corresponds to the fact that the source mechanism of the A-type earthquake is the strike-slip fault type whose directions of nodal planes are north-south and east-west. In contrast, vertical vector dipole ($\ddot{M}_{zz}$) is dominant for BH-type, BL-type and explosion earthquakes. The double-couple components ($\ddot{M}_{xy}$, $\ddot{M}_{xz}$ and $\ddot{M}_{yz}$) are less than 15% of the vertical dipole

component of BH-type, BL-type and explosion earthquakes, respectively. Horizontal dipole components are smaller than vertical one. On an average, horizontal dipole components of BH-type, BL-type and explosion earthquakes are 7%, 9% and 22% of the vertical dipole components, respectively.

Horizontal dipole components ($\ddot{M}_{xx}$ and $\ddot{M}_{yy}$) of a few BH-type earthquakes which are located at depths more than 2 km are exceptionally large. However, the $\ddot{M}_{xx}$ and $\ddot{M}_{yy}$ contain errors of ±36~72%, and it is tentatively concluded that such a large horizontal dipole was caused by the error in estimation.

### 4-3 Vertical dipole model

Two important results are obtained from the analysis in relation to the source mechanism of BH-type, BL-type and explosion earthquakes. One is the dominance of SV-wave components and the other is that of a vertical dipole component deduced from the amplitude inversion of P-wave. These may permit us to model their source mechanism on a single dipole.

Assuming the source mechanism of a single dipole for BH-type, BL-type and explosion earthquakes, the most appropriate orientation of the dipole for the observation was determined. From Equation (3), the radiation function for a single dipole with arbitrary orientation is simplified as

$$F_P(\phi) = \ddot{M}_0 \cos^2 \phi, \tag{4}$$

where $M_0$ and $\phi$ are second derivative of moment of the dipole and an angle between the unit vector of the dipole **d** and position vector of a station **x**,

respectively. The angle $\phi$ is described as

$$\phi = \cos^{-1}\frac{\mathbf{x}\cdot\mathbf{d}}{|\mathbf{x}||\mathbf{d}|}. \tag{5}$$

Therefore, the particle velocity of P-waves generated by the single dipole is rewritten as

$$\dot{u}^P(\mathbf{x}) = \frac{\ddot{M}_0 \cos^2\phi \exp\left(-\frac{\omega r}{2V_P Q_P}\right)}{4\pi\rho V_P{}^3 r} \tag{6}$$

The orientation of the dipole was so determined that theoretical amplitudes of P-waves would fit the observed ones by rotating the direction of the unit vector d. The tilt angles from the vertical direction and the azimuths of the dipoles are shown in Table 4 and Fig. 11. The ranges of tilt angles are 5～17°, 6～17° and 1～11° for BH-type, BL-type and explosion earthquakes, respectively. The tilt angles are small. It is concluded that the source mechanisms of the onset of BH-type, BL-type and explosion earthquake are represented by a single dipole vertically oriented.

In order to assure the validity of the vertical dipole model, the fitness of theoretical amplitudes of P- and SV-waves to the observed ones was evaluated for BH-type, BL-type and explosion earthquakes.

The theoretical amplitudes of P-waves were estimated using Equations (2) and (4). The radiation function for the vertical dipole is obtained by replacing $\phi=\xi$ and $\ddot{M}_0=\ddot{M}_{zz}$ in Equation (4) and is described as

$$F_p(\xi) = \ddot{M}_{zz}\cos^2\xi. \tag{7}$$

For SV-waves, the theoretical amplitudes were estimated according to the same procedure. The amplitude of particle velocity of SV-wave is written as

$$\dot{u}^{SV}(\mathbf{x}) = \frac{F_{SV}(\theta,\xi)\exp\left(-\dfrac{\omega r}{2V_S Q_S}\right)}{4\pi\rho V_S^3 r}, \tag{8}$$

where $V_s$ and $Q_s$ are the propagation velocity of S-wave and $Q_s$-factor, respectively. $F_{SV}(\theta, \xi)$ is a function which represents the radiation pattern of SV-wave and is represented as

$$\begin{aligned} F_{SV}(\theta,\xi) = &-(\ddot{M}_{xx}\cos^2\theta + \ddot{M}_{yy}\sin^2\theta - \ddot{M}_{zz} + 2\ddot{M}_{xy}\sin\theta\cos\theta)\sin\xi\cos\xi \\ &+(\ddot{M}_{xz}\cos\theta + \ddot{M}_{yz}\sin\theta)(\sin^2\xi - \cos^2\xi). \end{aligned} \tag{9}$$

$F_{SV}(\theta, \xi)$ for the vertical dipole model is simplified as

$$F_{SV}(\xi) = \frac{1}{2}\ddot{M}_{xz}\sin 2\xi. \tag{10}$$

The theoretical amplitudes of P- and SV-waves generated by the vertical dipole were estimated assuming $Q_s$=20 (tentatively same as $Q_p$) and $V_s$=1.4 km/s. The theoretical amplitudes of P- and SV-wave were compared with the observed ones (Fig. 12). For the observed amplitudes of SV-wave, the ranges of amplitudes during 2 seconds after the expected arrival times of S-waves are plotted.

The discrepancy between the estimated and observed amplitudes of P-wave of the BH-type earthquake is less than 3% when normalized by the amplitude at station HIK. For BL-type earthquake, the discrepancy is less than 2%. In the case of explosion earthquake, it does not exceed 4% except at stations ARI and

GON. The amplitudes of P-wave coincide reasonably with the observed ones for BH-type, BL-type and explosion earthquakes.

The theoretical amplitudes of SV-wave are in the range of observed values. The amplitude distribution of SV-wave supports the vertical dipole model as a probable source mechanism of BH-type, BL-type and explosion earthquakes.

## 5. Discussion

### 5-1 Source mechanisms of volcanic earthquakes

Minakami (1974) and Nishi (1978) investigated the polarity distribution of A-type earthquakes and showed that the push-pull pattern was of the quadrant type, similarly to tectonic ones. Through the analysis in the present study, it is confirmed that components of double couple are dominant in A-type earthquakes. This result is consistent with that of the previous studies.

A model of isotropic expansion has been applied to the mechanism of explosion earthquakes at Sakurajima and Asama volcanoes (Nishi, 1980; Imai, 1980). Isotropic expansion is equivalent to three mutually perpendicular vector dipoles (Aki and Richards, 1980). However, the analysis in the present study showed that three vector dipoles are not comparable to each other, but the vertical dipole is dominant. This result is consistent with the vertically polarized S-waves. It is concluded that the source mechanism of explosion earthquakes is not a type of isotropic expansion but that of expansion dominant in the vertical direction. Both BH-type and BL-type earthquakes have a vertical expansion source similar to explosion earthquakes as revealed in the present study.

Similarity between BH-type, BL-type and explosion earthquakes is also recognized in their frequency contents. These three types of earthquakes are commonly lacking in high-frequency components of more than 10 Hz. On the other hand, A-type earthquakes have dominant high frequency contents of 10 to 20 Hz. The difference between A-type earthquakes and the other three types may be attributed to the difference in their hypocentral locations.

Ishihara (1990) inferred that the hypocentral zone of explosion earthquakes corresponds to a part of volcanic conduit, but A-type earthquakes are originated in the surrounding brittle rocks based on the difference in hypocentral locations and spectra between A-type and explosion earthquakes. The hypocentral zones of BH-type and BL-type earthquakes almost coincide with that of explosion earthquakes. The precise determination of hypocenters allows us to conclude that both BH-type and BL-type earthquakes also occur in the conduit.

A-type earthquakes have a faulting source and are generated by a release of shear strain. The shear strain cannot be accumulated in the conduit filled with magma but in competent rocks. Therefore, A-type earthquakes should occur by shear fracture of rocks around the conduit.

On the other hand, source mechanism of BH-type, BL-type and explosion earthquakes is described by a vertical dipole which is necessarily accompanied by a vertical expansion of sources. In a recent activity of Sakurajima Volcano, lava dome has sometimes been observed in the summit crater and it is inferred that the conduit has been filled with magma. Under such a condition, volume strains may be accumulated in the conduit, probably near the boundary of lava and volcanic

gases separated from magma. The vertically elongated conduit may control the direction of expansion. It is probable that BH-type, BL-type and explosion earthquakes are caused by the release of volume strain related to the expansion process of a gas pocket along the conduit. Some BL-type earthquakes have all dilatational arrivals which might have been caused by the disruption of gas pockets.

The dominant frequencies of BH-type, BL-type and explosion earthquakes are different from each other, though they have a similar source mechanism. As these three types of earthquakes coexist at depths from 2 to 3 km beneath the crater, the difference in dominant frequencies may not be due to the effect of propagation path but rather to the effect of source processes.

Previous studies have clarified that these three types of volcanic earthquakes are originated in different stages of volcanic activity (Ishihara, 1985; Ishihara and Iguchi, 1989; Kamo and Ishihara, 1989). The difference in their source processes might be affected by the state of magma conduit. Volcanic activity related to these earthquakes and inferred states of the magma conduit are summarized in Table 5 and are schematically illustrated in Fig. 13.

BH-type earthquakes are originated when magma intrusion starts after a dormant period of several months. At that time, the conduit is thought to have been occupied by partially solidified lava due to cooling as shown in Fig. 13(a). While BL-type earthquakes swarm, volcanic bombs, ashes and gases are intermittently ejected from the vent at the crater. This phenomenon suggests that the conduit is filled with fluid magma as shown in Fig. 13(b). While BH-type earthquakes occur, the viscosity and yield strength of magma in the conduit are inferred to be

higher than those during swarms of BL-type earthquakes. In such states of the conduit, expansion process of BH-type earthquakes are probably terminated in a shorter time than that of BL-type earthquakes. This may be one of the reasons why BH-type earthquakes have higher-frequency components than BL-type earthquakes.

Explosive eruptions are generated by intrusion of magma and partly due to degassing of magma after lava domes have been formed (Ishihara, 1990). Before explosion earthquakes occur, the conduit is filled with a mixture of viscous magma and gases, and the top of the conduit is closed by lava domes as shown in Fig. 13(c). This suggests that magma and gases are confined in the conduit with a higher pressure than that while the swarms of BL-type earthquakes. More impulsive onset, larger amplitudes and lower-frequency components of explosion earthquakes than those of BL-type earthquakes might be attributed to the release of higher pressure accumulated in a larger gas pocket.

The difference in states of magma conduit is probably the main factor controlling the source process of BH-type, BL-type and explosion earthquakes. However, we cannot discuss further about this problem because the present analysis has been focused only on the first motions of P-waves, and the whole process of volcanic earthquakes has not been examined. To clarify the whole process, later phases should be analyzed. The appearance of transverse shear waves 1～2 seconds after the SV-waves would provide important information, since they suggest horizontal forces exerted after the vertical expansion.

### 5-2 Comparison with other volcanoes

At Aso and Miyakejima volcanoes, the source mechanisms of volcanic earthquakes whose waveforms are similar to those of BH-type and BL-type earthquakes have been studied by investigating the distribution of the first motions of P-waves. Source models different from those of the BH-type and BL-type earthquakes at Sakurajima Volcano have been proposed.

Wada (1989) showed that the source mechanism of the low frequency earthquakes associated with eruptive activity in 1979 and 1980 at Aso Volcano was of the quadrant type and the P-axis was oriented near vertically. He suggested that the earthquakes were generated by fracturing of rocks around a gas chamber and that the low frequency was attributed to low yield strength. The difference in source mechanisms between the B-type earthquakes at Sakurajima Volcano and the earthquakes at Aso may be attributed to the condition in the conduit. At Sakurajima Volcano, eruptive activity at the summit crater has continued for more than 30 years and the conduit has been steadily filled with magma. By contrast, Aso Volcano has recently repeated phreatic and phreatomagmatic eruptions in a time interval of a few to ten years, and it is inferred that the conduit is not filled thoroughly with liquid magma. Concerning the source mechanisms of volcanic earthquakes at both volcanoes, a common feature is found that the principal stress axis is oriented vertically.

Related to the 1983 fissure eruption at Miyakejima Volcano, Shimizu *et al.* (1987) found that explosive and implosive short-period earthquakes had distinct S-waves. To explain these peculiar nature, they proposed a model of a combination

of shear and tensile cracks, and found that the direction of tensile cracks almost coincided with that of fissure zone on the ground surface. They interpreted that the earthquakes were generated by opening and closing of a crack, driven by basaltic magma intrusion and drain back, respectively. The difference in source mechanisms between BH-type earthquakes at Sakurajima Volcano and the earthquakes at Miyakejima is mainly due to the shape of magma path: a vertical conduit at Sakurajima Volcano and a laterally extended fissure at Miyakejima.

The comparison of source mechanism of volcanic earthquakes at Sakurajima Volcano with those at Aso and Miyakejima suggests that the source mechanism is not unique, but it depends on both the level of activity and the shape of magma path.

## 6. Conclusions

Volcanic earthquakes at Sakurajima Volcano are classified into A-type, BH-type, BL-type and explosion earthquakes, and their source mechanisms are investigated by analyzing seismograms obtained mainly by borehole seismometers. The principal conclusions are:

1) The precise determination of hypocenters shows that BH-type, BL-type and explosion earthquakes are distributed in a cylindrical zone with a radius of about 200 m beneath the crater. The amplitude inversion of second derivative of moment tensor revealed that the source mechanisms of BH-type, BL-type and explosion earthquakes are of the vertical expansion type. These three types of earthquakes may be originated by the expansion of a gas pocket in the cylindrical conduit filled with magma. By contrast, A-type earthquakes are originated around

the conduit and have dominant double-couple component. A-type earthquakes are thought to be originated by shear fracturing of the brittle rocks around the conduit.

2) Considering the eruptive activity and ground deformation related to these three types of earthquakes, the most probable factor affecting the dominant frequency of BH-type, BL-type and explosion earthquakes is the state of the magma conduit.

3) The source mechanisms of BH-type and BL-type earthquakes at Sakurajima Volcano differ from those of volcanic earthquakes at Aso and Miyakejima. Considering the difference in eruption styles at these volcanoes, it is inferred that the source mechanism of volcanic earthquakes depends on both the level of activity and the structure of magma conduits.

**Acknowledgments**

The author would like to appreciate Professors Kosuke Kamo, Ichiro Nakagawa and Kazuhiro Ishihara of Kyoto University for their encouragement and helpful suggestions. Dr. Gillian Foulger of U. S. Geological Survey, Professor Bor-Ming Jahn of Rennes University, France and Professors Yasuaki Sudo, Yoshimasa Kobayashi and Yoshiyuki Tatsumi of Kyoto University read this manuscript and gave useful suggestions. Professors Kazuo Oike and Masataka Ando of Kyoto University, Dr. Michael P. Ryan of U. S. Geological Survey and staff members of Sakurajima Volcanological Observatory and Aso Volcanological Laboratory of Kyoto University gave discussion and helpful comments.

## References


Aki, K. and Richards, P G. (1980) Quantitative Seismology. W. H. Freeman and Company, San Francisco.

Barquero, R., Alvarado, G. E. and Matumoto, T. (1992) Arenal Volcano (Costa Rica) premonitory seismicity. In *Volcanic Seismology, IAVCEI Proc. 3*, (Gasparini, P., Scarpa, R. and Aki, K. eds), 84−96. Springer-Verlag.

Endo, E. T., Malone, S. D., Noson, L. L. and Weaver, C. S. (1981) Locations, magnitudes, and statistics of the March 20 − May 18 earthquake sequence. *U.S. Geol. Surv. Prof. Pap.*, **1250**, 93−107.

Iguchi, M. (1985) Analysis of volcanic "shallow earthquakes" observed near the active crater. *Bull. Volcanol. Soc. Japan*, **30**, 1−10 (in Japanese).

Iguchi, M. (1989) Distribution of the initial motions of volcanic microearthquakes (B-type) at Sakurajima Volcano. *Ann. Disas. Prev. Res. Inst., Kyoto Univ.*, **32B-1**, 13−22 (in Japanese).

Iguchi, M. (1991) Geophysical data collection using an interactive personal computer system (Part 1) −Experimental monitoring at Suwanosejima Volcano− *Bull. Volcanol. Soc. Japan*, **35**, 335−343.

Imai, H. (1980) Explosion earthquakes associated with the 1973 eruptions of Asama Volcano. (Part II) The summary of studies on explosion earthquakes and a model of explosive eruptions inferred from seismic data. *Bull. Earthq. Res. Inst., Univ. Tokyo*, **55**, 537−576 (in Japanese).

Ishihara, K. (1985) Dynamical analysis of volcanic explosion. *J. Geodyn.*, **3**, 327−349.

Ishihara, K. (1990) Pressure sources and induced ground deformation associated with explosive eruptions at an andesitic volcano, Sakurajima Volcano, Japan. In *Magma Transport and Storage* (Ryan, M. P ed), 335−356. John Wiley & Sons.

Ishihara, K. and Iguchi, M. (1989) The relationship between micro-earthquake swarms and volcanic activity at Sakurajima Volcano. *Ann. Disas. Prev. Res. Inst., Kyoto Univ.*, **32B-1**, 1−11 (in Japanese).

Kamo, K. (1978) Some phenomena before the summit eruptions at Sakura-zima Volcano. *Bull. Volcanol. Soc. Japan*, **23**, 53−64 (in Japanese).

Kamo, K. and Ishihara, K. (1989) A preliminary experiment on automated judgement of the stages of eruptive activity using tiltmeter records at Sakurajima, Japan. In *Volcanic Hazards, IAVCEI Proc. 1* (Latter, J. H. ed), 585−598. Springer-Verlag.

Latter, J. H. (1981) Volcanic earthquakes, and their relationship to eruptions at Ruapehu and Ngauruhoe Volcanoes. *J. Volcanol. Geotherm. Res.*, **9**, 293−309.

Malone, S. D. (1983) Volcanic earthquakes, examples from Mt. St. Helens. In *Earthquakes, Observation, Theory and Interpretation* (Kanamori, H. ed), 435−455. North-Holland.

McNutt, S. R. (1986) Observations and analysis of B-type earthquakes, explosions, and volcanic tremor at Pavlof Volcano, Alaska. *Bull. Seism. Soc. Am.*, **76**, 153−175.

Minakami, T. (1970) Seismometrical studies of volcano Asama Part 1. *Bull.Earthq. Res. Inst., Univ. Tokyo*, **48**, 235−301.

Minakami, T. (1974) Seismology and volcanoes in Japan. In *Physical Volcanology*

(Civetta, L., Gasparini, P., Luongo, G., Rapolla, A. eds), 1−27. Elsevier, New York.

Montalbetti, J. F and Kanasewich, E. R. (1970) Enhancement of teleseismic body phases with a polarization filter. *Geophys. J. R. astr. Soc.*, **21**, 119−129.

Nishi, K. (1978) On the focal mechanism of volcanic earthquakes in Sakurajima Volcano. *Ann. Disas. Prev. Res. Inst., Kyoto Univ.*, **21**, 145−152 (in Japanese).

Nishi, K. (1980) Spectral study on the volcanic earthquake(1) −Explosion earthquake− *Ann. Disas. Prev. Res. Inst., Kyoto Univ.*, **23B-1**, 29−35 (in Japanese).

Shimizu, H., Ueki, S. and Koyama, J. (1987) A tensile-shear crack model for the mechanism of volcanic earthquakes. *Tectonophys.*, **144**, 287−300.

Shimozuru, D. and Kagiyama, T. (1989) Some significant features of pre-eruption volcanic earthquakes. In *Volcanic Hazards, IAVCEI Proc. 1* (Latter, J. H. ed), 504−512. Springer-Verlag.

Sudo, Y. (1991) An attenuating structure beneath the Aso Caldera determined from the propagation of seismic waves. *Bull. Volcanol.*, **53**, 99−111.

Wada, T. (1989) Focal mechanism of volcanic earthquakes. *Ann. Disas. Prev. Res. Inst., Kyoto Univ.*, **32B-1**, 23−28 (in Japanese).

Yamasato, H. (1987) Distribution of the initial motions of explosion earthquakes at Sakurajima Volcano. *Bull. Volcanol. Soc. Japan*, **32**, 289−300 (in Japanese).

Yoshikawa, K. and Nishi, K. (1965) Seismic observation at the Volcano Sakurajima (4). *Ann. Disas. Prev. Res. Inst., Kyoto Univ.*, **8**, 51−57 (in Japanese).

Table 1. Specification of seismometers.

| Station code | Distance from the crater (km) | Type of seismometer | Depth (m) | Component | Natural frequency (Hz) | Damping factor |
|---|---|---|---|---|---|---|
| HIK | 1.7 | Ground-based | 2 | V[2], L[3], T[4] | 1.0 | 1.0 |
| FUR[1] | 1.7 | Ground-based | 2 | V, L, T | 1.0 | 1.0 |
| ARI[1] | 2.7 | Borehole | 85 | V, L, T | 1.0 | 1.0 |
| GON | 2.3 | Ground-based | 2 | V, L, T | 1.0 | 1.0 |
| NOJ | 2.9 | Ground-based | 0 | V | 1.0 | 1.0 |
| HAR | 2.8 | Borehole | 290 | V, L, T | 1.0 | 1.0 |
| KAB | 3.3 | Borehole | 143 | V, L, T | 1.0 | 1.0 |
| KOM | 4.4 | Borehole | 90 | V, L, T | 1.0 | 1.0 |
| KOI | 4.5 | Ground-based | 2 | V | 1.0 | 1.0 |

1) Station FUR was replaced by station ARI in January 1988.

2) V:Vertical component

3) L:Horizontal component in the direction to the crater

4) T:Horizontal component in the direction perpendicular to the crater

Table 2. Hypocentral location and amplitude of the first motion of P-wave.

| Date | Time | Type | Hypocenter (km) | | | Amplitude of the first motion of P-wave (μm/s) | | | | | | | | |
|---|---|---|---|---|---|---|---|---|---|---|---|---|---|---|
| | | | E-W | N-S | Depth | HIK | FUR | ARI | GON | NOJ | HAR | KAB | KOM | KOI |
| Correction factor | | | | | | 1.69 | 1.85 | 2.56 | 1.08 | 1.47 | 4.55 | 4.55 | 4.34 | 1.00 |
| 1988-04-15 | 00:59 | EX | -0.10 | 0.14 | 1.91 | 144 | | 43 | 43 | 41 | 50 | 41 | 14 | 7 |
| 1988-04-20 | 08:36 | EX | 0.00 | 0.18 | 1.89 | 176 | | 40 | 29 | 34 | 40 | 37 | 12 | 6 |
| 1988-04-24 | 23:49 | EX | -0.01 | 0.25 | 1.61 | 50 | | 30 | 25 | 21 | 32 | 30 | 12 | 5 |
| 1988-05-11 | 06:28 | EX | -0.12 | 0.33 | 2.00 | 250 | | 77 | 55 | 69 | 94 | 70 | 31 | 14 |
| 1988-05-13 | 02:06 | EX | -0.12 | 0.16 | 1.44 | 68 | | 21 | 7 | 17 | 14 | 16 | 5 | 2 |
| 1988-03-11 | 01:48 | BL | 0.10 | 0.16 | 1.64 | 17 | | 4 | 4 | 2 | 6 | 3 | 3 | 1 |
| 1988-03-13 | 23:23 | BL | -0.17 | 0.21 | 1.52 | 25 | | 7 | 3 | 6 | 5 | 4 | 3 | 1 |
| 1988-04-07 | 22:17 | BL | -0.14 | 0.13 | 1.55 | 71 | | 7 | 6 | 10 | 8 | 5 | 3 | 2 |
| 1988-07-02 | 00:17 | BL | -0.06 | 0.11 | 1.31 | 22 | | 6 | 5 | 6 | 7 | 8 | 3 | 2 |
| 1988-08-04 | 18:56 | BL | -0.14 | 0.25 | 1.41 | 37 | | 8 | 8 | 11 | 11 | 7 | 2 | 2 |
| 1988-10-23 | 00:30 | BL | -0.04 | 0.15 | 1.36 | 26 | | 13 | 9 | 13 | 16 | 13 | 5 | 3 |
| 1988-09-03 | 21:50 | BL | -0.03 | 0.16 | 1.38 | -20 | | -3 | -1 | -5 | -8 | -3 | -3 | -2 |
| 1987-09-04 | 07:45 | BH | -0.12 | 0.36 | 1.84 | 44 | 27 | | 5 | 8 | 7 | 3 | 1 | 2 |
| 1987-09-04 | 12:08 | BH | -0.10 | 0.38 | 2.66 | 125 | 61 | | 4 | 17 | 13 | 5 | 2 | 1 |
| 1987-09-04 | 19:43 | BH | -0.19 | 0.32 | 1.32 | 50 | 18 | | 3 | 6 | 7 | 3 | 2 | 1 |
| 1987-09-04 | 23:40 | BH | -0.29 | 0.41 | 1.76 | 49 | 24 | | 1 | 6 | 5 | 3 | 2 | 1 |
| 1987-10-16 | 22:20 | BH | -0.04 | 0.45 | 1.59 | 31 | 22 | | 11 | 5 | 6 | 3 | 1 | 2 |
| 1987-10-17 | 03:21 | BH | -0.17 | 0.34 | 1.39 | 39 | 15 | | 6 | 5 | 4 | 2 | 2 | 1 |
| 1988-05-03 | 18:44 | BH | -0.04 | 0.20 | 2.43 | 103 | | 25 | 16 | 19 | 17 | 8 | 2 | 4 |
| 1988-05-19 | 12:29 | A | -0.25 | -0.09 | 3.59 | 11 | | 2 | 4 | -56 | 44 | 24 | -3 | 17 |
| 1988-05-19 | 12:38 | A | -0.32 | 0.03 | 4.04 | 63 | | 65 | -6 | -141 | 161 | 105 | -11 | 8 |

Table 3. Components of second derivative of moment tensor.

| Date | Time | Type | Second derivative of moment ($\times 10^{14}$Nm/s$^2$) | | | | | |
|---|---|---|---|---|---|---|---|---|
| | | | $\ddot{M}_{xx}$ | $\ddot{M}_{yy}$ | $\ddot{M}_{zz}$ | $\ddot{M}_{xy}$ | $\ddot{M}_{xz}$ | $\ddot{M}_{yz}$ |
| 1988-04-15 | 00:59 | EX | -0.61 | -0.02 | 3.15 | 0.04 | -0.26 | 0.27 |
| 1988-04-20 | 08:36 | EX | -1.12 | -0.33 | 3.72 | 0.17 | -0.55 | 0.33 |
| 1988-04-24 | 23:49 | EX | 0.01 | 0.49 | 1.17 | -0.11 | -0.05 | 0.11 |
| 1988-05-11 | 06:28 | EX | -1.19 | 0.18 | 5.19 | 0.26 | -0.60 | 0.33 |
| 1988-05-13 | 02:06 | EX | -0.26 | 0.13 | 1.37 | 0.02 | -0.16 | 0.05 |
| Normalized average | | | -0.18 | +0.09 | +1.00 | +0.01 | -0.10 | +0.07 |
| Error | | | ±0.06 | ±0.07 | ±0.08 | ±0.05 | ±0.04 | ±0.03 |
| 1988-03-11 | 01:48 | BL | -0.06 | 0.04 | 0.48 | 0.03 | -0.07 | 0.10 |
| 1988-03-13 | 23:23 | BL | -0.06 | 0.08 | 0.63 | 0.05 | -0.06 | 0.03 |
| 1988-04-07 | 22:17 | BL | -0.38 | -0.28 | 1.89 | 0.16 | -0.23 | 0.13 |
| 1988-07-02 | 00:17 | BL | -0.02 | 0.14 | 0.58 | 0.00 | -0.07 | 0.09 |
| 1988-08-04 | 18:56 | BL | 0.00 | 0.05 | 0.93 | 0.04 | -0.11 | 0.01 |
| 1988-10-23 | 00:30 | BL | 0.11 | 0.39 | 0.62 | -0.01 | -0.11 | 0.08 |
| 1988-09-03 | 21:50 | BL | 0.00 | -0.07 | -0.40 | -0.06 | 0.13 | -0.09 |
| Normalized average* | | | -0.05 | +0.16 | +1.00 | +0.04 | -0.13 | +0.10 |
| Error | | | ±0.09 | ±0.08 | ±0.13 | ±0.06 | ±0.06 | ±0.03 |
| 1987-09-04 | 07:45 | BH | -0.33 | -0.34 | 2.85 | 0.23 | -0.41 | -0.25 |
| 1987-09-04 | 12:08 | BH | -8.42 | -8.58 | 12.87 | 4.48 | -2.92 | 0.60 |
| 1987-09-04 | 19:43 | BH | -0.19 | -0.08 | 2.45 | 0.34 | -0.34 | 0.15 |
| 1987-09-04 | 23:40 | BH | -0.62 | -0.29 | 2.81 | 0.33 | -0.30 | -0.13 |
| 1987-10-16 | 22:20 | BH | 0.28 | -0.11 | 1.99 | -0.08 | -0.03 | -0.36 |
| 1987-10-17 | 03:21 | BH | -0.15 | -0.21 | 2.18 | 0.27 | -0.15 | 0.08 |
| 1988-05-03 | 18:44 | BH | -3.08 | -3.41 | 9.30 | 1.05 | -1.52 | 0.02 |
| Normalized average | | | -0.19 | -0.21 | +1.00 | +0.13 | -0.12 | -0.02 |
| Error | | | ±0.13 | ±0.22 | ±0.17 | ±0.15 | ±0.12 | ±0.10 |
| 1988-05-19 | 12:29 | A | 0.25 | 0.19 | -0.09 | -1.98 | 0.28 | 0.76 |
| 1988-05-19 | 12:38 | A | -4.24 | 2.53 | 1.69 | -8.61 | 1.18 | 2.60 |

Numbers with underline represent the maximum value among six components.

* Not including the implosive BL event on September 3, 1988.

Table 4. Tilt and azimuth of the dipole.

| Date | Time | Type | Tilt (°) | Azimuth (°) |
|---|---|---|---|---|
| 1988-04-15 | 00:59 | EX | 7 | 295 |
| 1988-04-20 | 08:36 | EX | 11 | 281 |
| 1988-04-24 | 23:49 | EX | 1 | 284 |
| 1988-05-11 | 06:28 | EX | 8 | 268 |
| 1988-05-13 | 02:06 | EX | 8 | 256 |
| | | | | |
| 1988-03-11 | 01:48 | BL | 12 | 304 |
| 1988-03-13 | 23:23 | BL | 7 | 249 |
| 1988-04-07 | 22:17 | BL | 9 | 285 |
| 1988-07-02 | 00:17 | BL | 6 | 298 |
| 1988-08-04 | 18:56 | BL | 7 | 256 |
| 1988-10-23 | 00:30 | BL | 8 | 219 |
| 1988-09-03 | 21:50 | BL | 17 | 279 |
| | | | | |
| 1987-09-04 | 07:45 | BH | 12 | 235 |
| 1987-09-04 | 12:08 | BH | 17 | 254 |
| 1987-09-04 | 19:43 | BH | 9 | 262 |
| 1987-09-04 | 23:40 | BH | 11 | 227 |
| 1987-10-16 | 22:20 | BH | 7 | 193 |
| 1987-10-17 | 03:21 | BH | 5 | 266 |
| 1988-05-03 | 18:44 | BH | 11 | 311 |

Table 5. Volcanic activity related to three types of volcanic earthquakes and inferred states of the magma conduit.

| Type of volcanic earthquake | BH-type earthquake | BL-type earthquake | Explosion earthquake |
|---|---|---|---|
| Eruptive activity | No significant activity[1)] | Effusive eruption[1)] | Explosive eruption |
| Ground deformation | Inflation[1)] | Deflation[1)] | Inflation prior to explosion and deflation after explosion[2)] |
| Magma process | Intrusion to the conduit[1)] | Effusive extrusion up to crater bottom[1)] | Explosive discharge of magma product |
| State of the upper part of the conduit | Close | Open | Closed by a cap of lava prior to explosion and open after it[3)] |
| State in the conduit | Occupied by partially solidified lava | Filled with fluidal lava up to the crater bottom | Gas chamber with high pressure[3)] |

1) Ishihara and Iguchi (1989), 2) Kamo and Ishihara (1989), 3) Ishihara (1985)

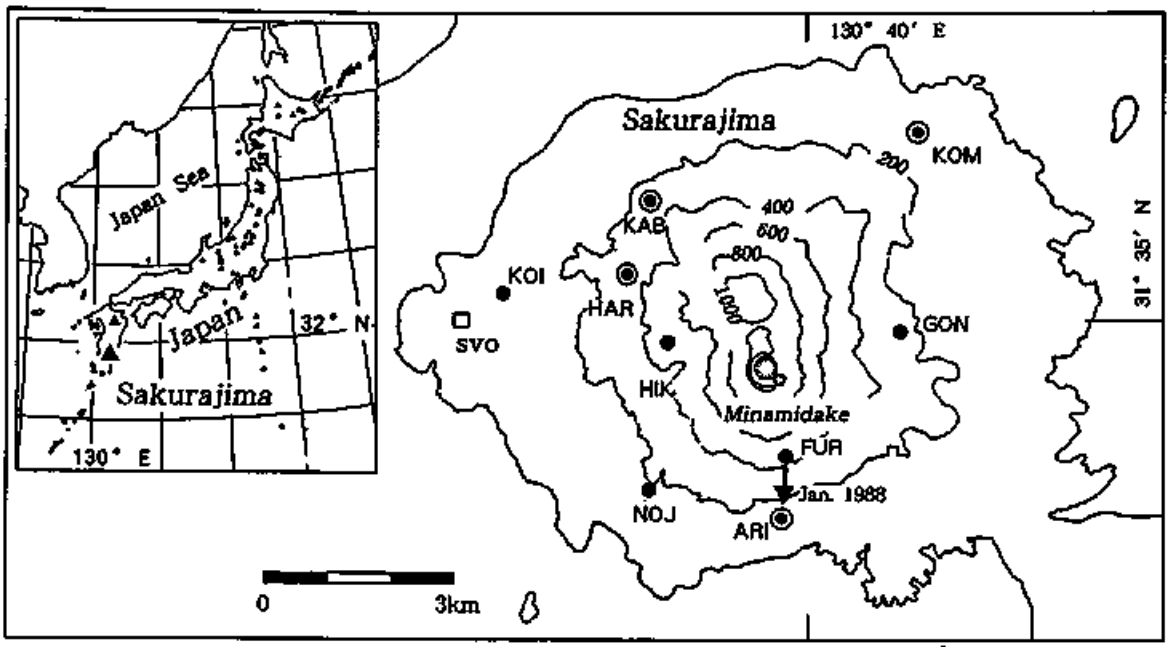


Fig. 1. Locations of seismic stations employed in the present study. Circles with solid dots and solid dots denote borehole seismometers of 3-components and seismometers installed on the ground surface, respectively. A square represents the Sakurajima Volcanological Observatory (SVO) where seismic signals from all stations are recorded.

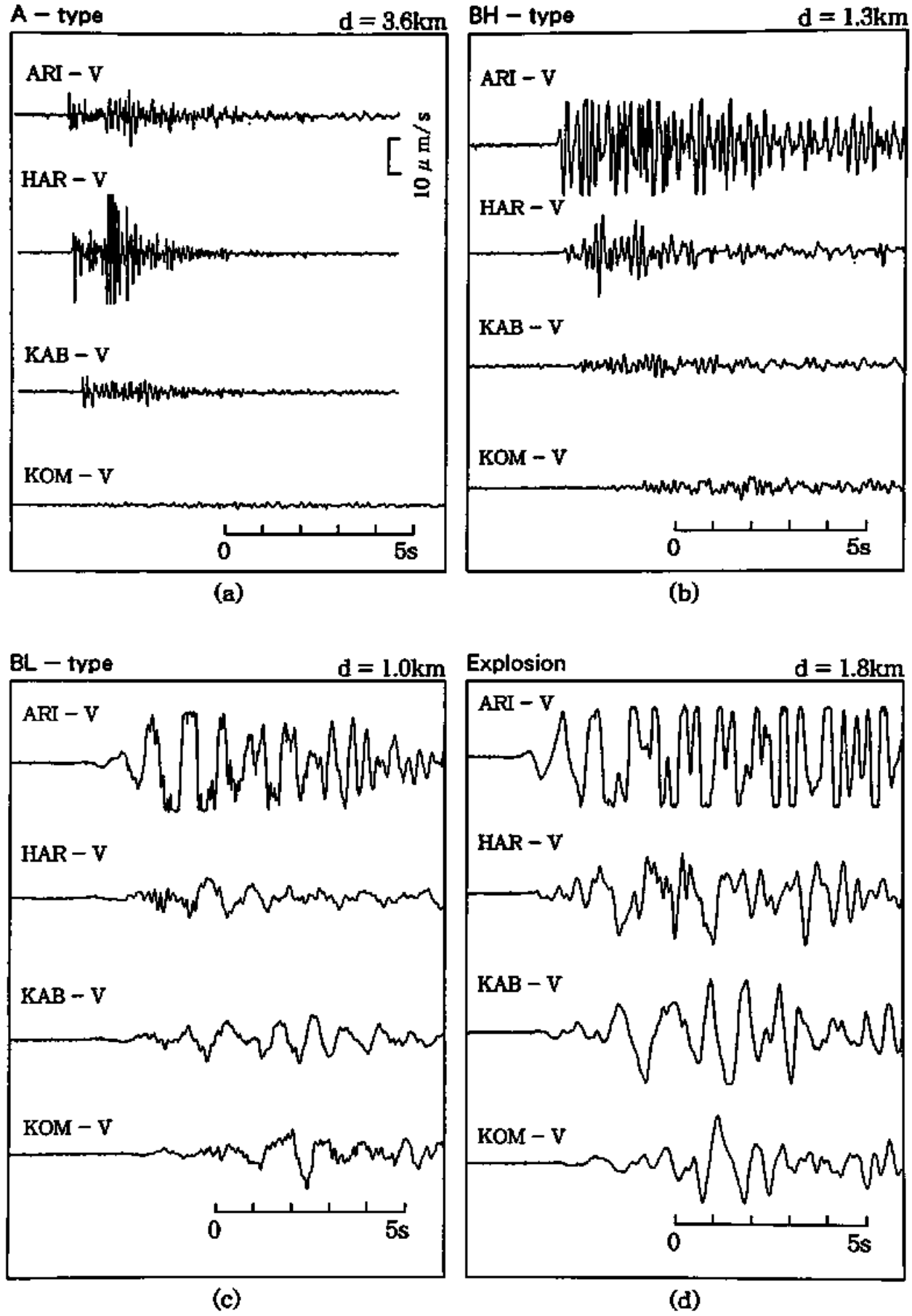


Fig. 2. Examples of seismograms of volcanic earthquakes. (a) A-type earthquake at 12:29, May 19, 1988, (b) BH-type earthquake at 12:08, September 4, 1987, (c) BL-type earthquake at 17:28, September 10, 1988 and (d) explosion earthquake at 23:59, June 4, 1988. Seismograms were obtained by borehole seismometers of vertical component at stations ARI, HAR, KAB and KOM which are located 2.7, 2.8, 3.3 and 4.4 km from the summit crater, respectively.

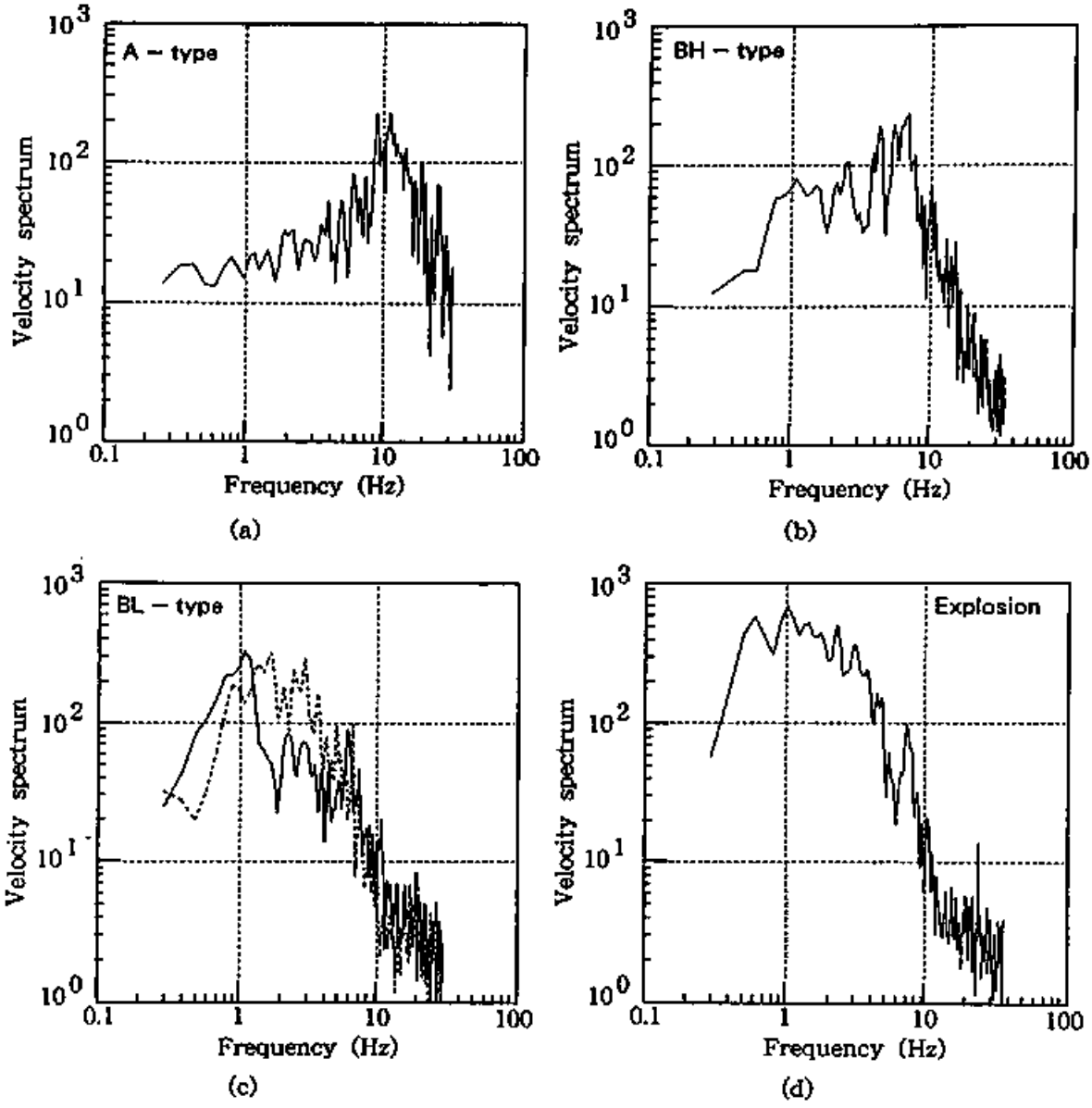


Fig. 3. Velocity spectra of volcanic earthquakes. 1,000 digits of the velocity spectrum are equivalent to 16 μm/s/Hz. (a) A-type earthquake at 12:29, May 19, 1988, (b) BH-type earthquake at 12:08, September 4, 1987, (c) BL-type earthquakes at 17:28, September 10, 1988 (solid line) and at 07:32, August 13, 1988 (broken line) and (d) explosion earthquake at 23:59, June 4, 1988.

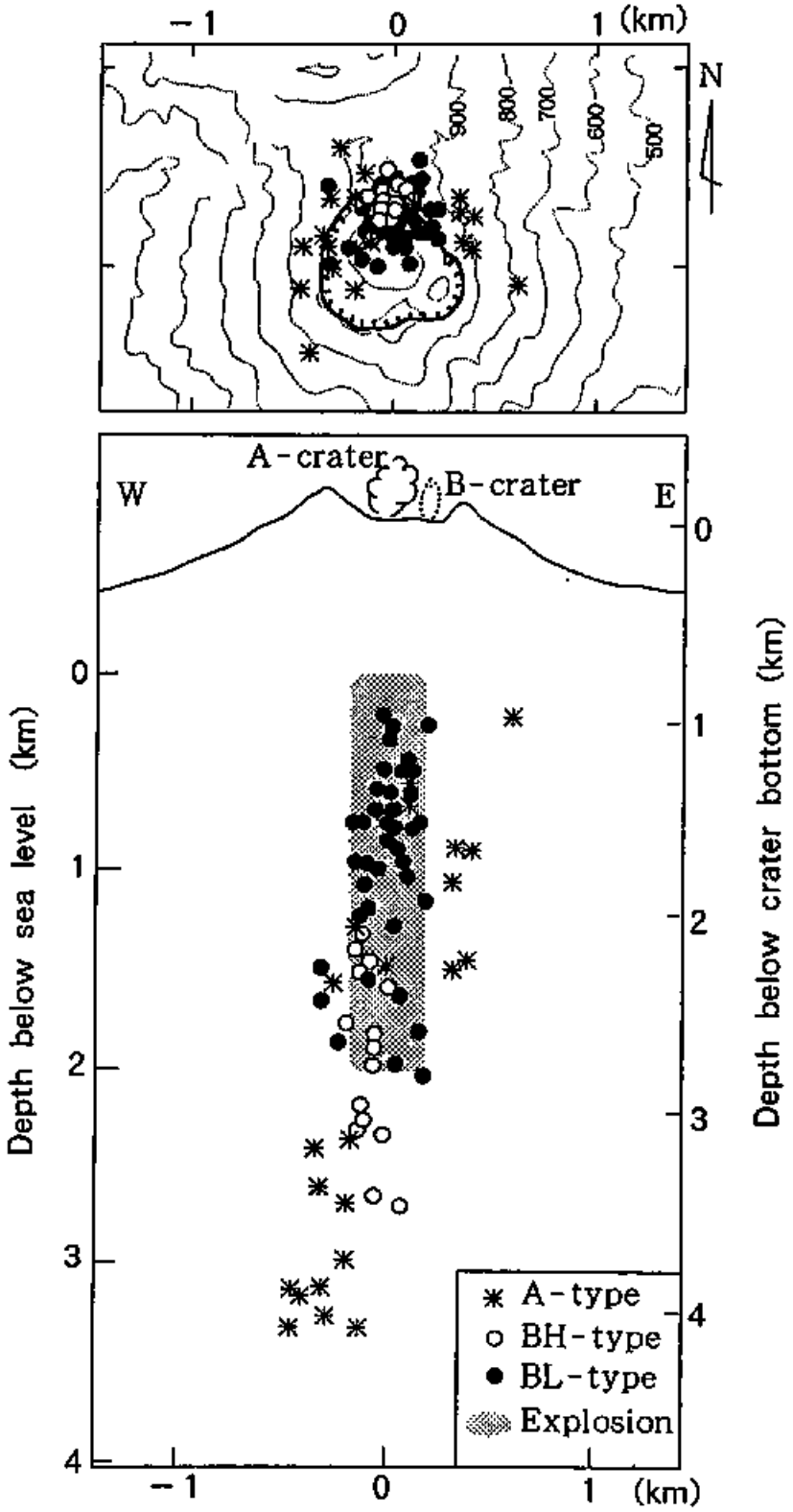


Fig. 4. Hypocentral distribution of volcanic earthquakes beneath the crater. Open and solid circles represent the locations of BH-type and BL-type earthquakes, respectively. A shaded area shows the focal zone of explosion earthquakes determined in the present study and also referred to Kamo (1978) and Ishihara (1990). Asterisks denote the locations of A-type earthquakes referred to Ishihara (1990).

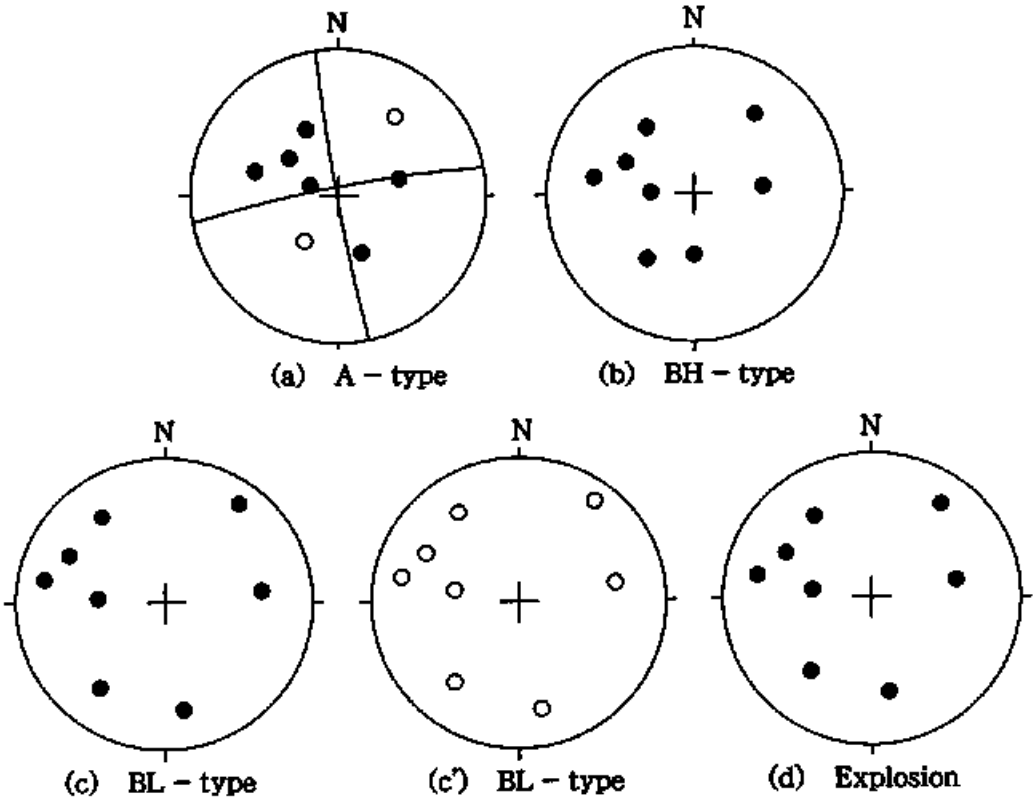


Fig. 5. Polarity distribution of the first motions of P-waves. Open and solid circles represent dilatational and compressional arrivals, respectively. These diagrams are equal-area projections on the upper hemispheres of the focal spheres. (a) A-type earthquake at 12:29, May 19, 1988. The focal sphere is divided into four quadrants. (b) BH-type earthquake at 12:08, September 4, 1987. (c) BL-type earthquake at 17:28, September 10, 1988, (c') BL-type earthquake at 11:26, April 25, 1988. First motions are dilatational at all stations. (d) Explosion earthquake at 00:59, April 15, 1988.

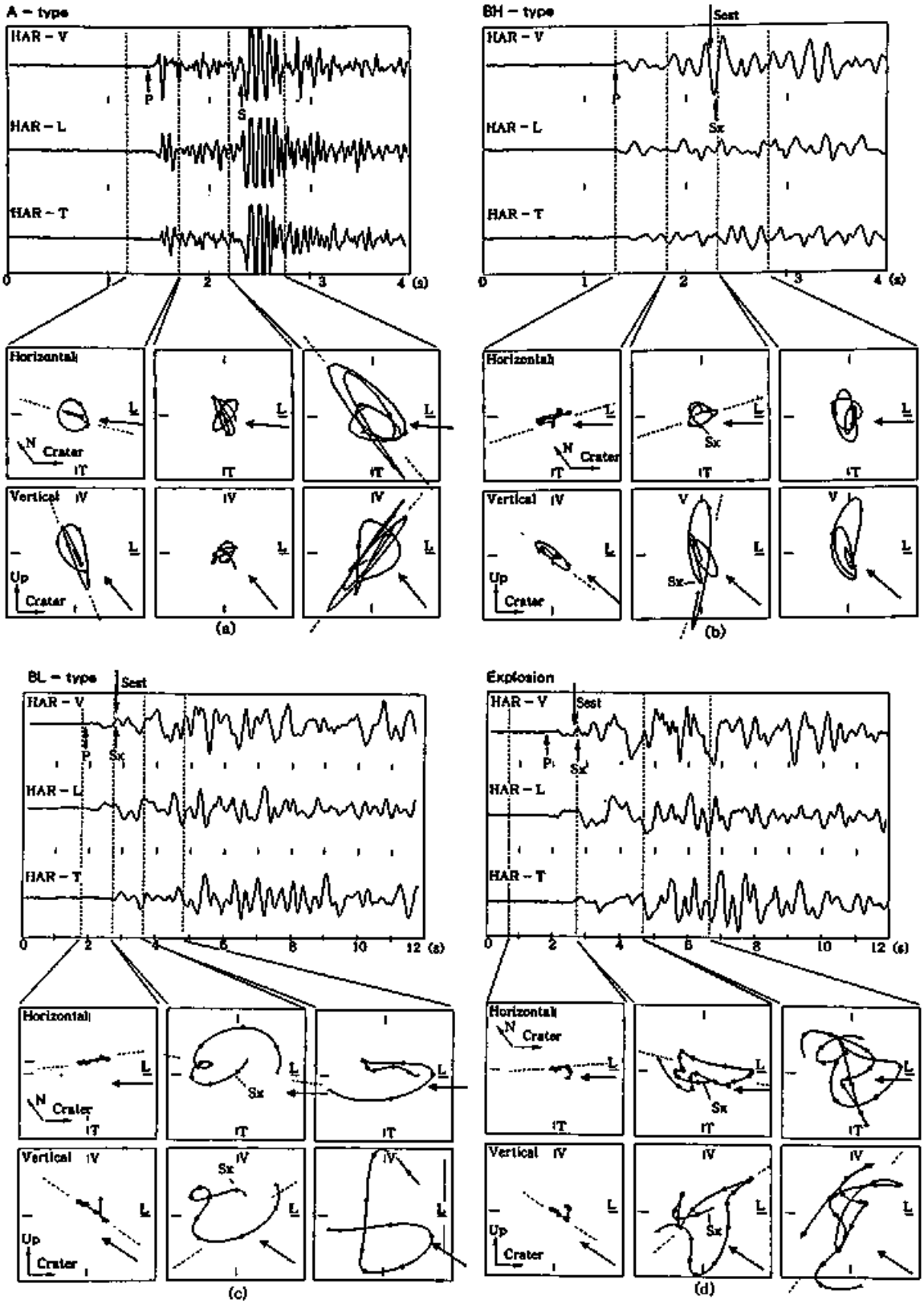


Fig. 6. Particle motion diagrams. The upper three traces represent particle ground velocities in the vertical, radial and tangential directions at station HAR. Motions on the horizontal plane and vertical cross-section in the direction of wave propagation are shown in the lower part of the diagrams. Circles are plotted every 0.1 second. Arrows represent the propagation direction of the first motions of P-waves reduced from hypocentral locations. The symbols "Sest" and "Sx" represent arrival times of S-waves estimated from focal distance and the beginning time of polarization perpendicular to the wave propagation, respectively. (a) A-type earthquake at 12:29, May 19, 1988, (b) BH-type earthquake at 12:08, September 4, 1987, (c) BL-type earthquake at 00:17, July 2, 1988 and (d) explosion earthquake at 23:59, June 4, 1988.

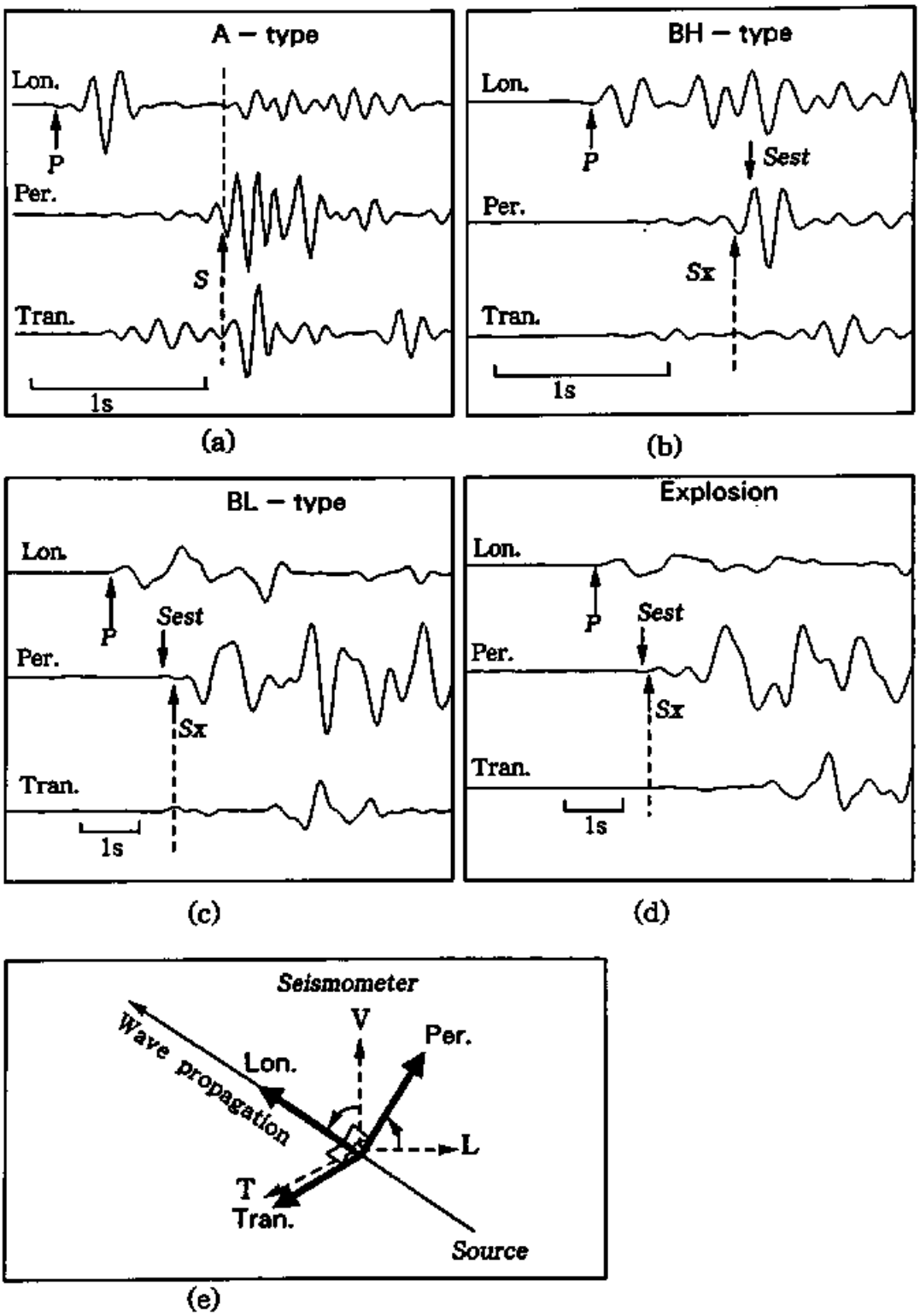


Fig. 7. Seismograms processed by applying a polarization filter. After the rotation of vertical and longitudinal components as shown in (e), the traces of "Lon.", "Per." and "Tran." correspond to the motions of P-wave, SV-wave and SH-wave, respectively. The symbols "Sest" and "Sx" represent arrival times of S-waves estimated from focal distances and from the beginning times of SV-wave component, respectively. (a) A-type earthquake at 12:29, May 19, 1988, (b) BH-type earthquake at 12:08, September 4, 1987, (c) BL-type earthquake at 00:17, July 2, 1988, (d) explosion earthquake at 23:59, June 4, 1988.

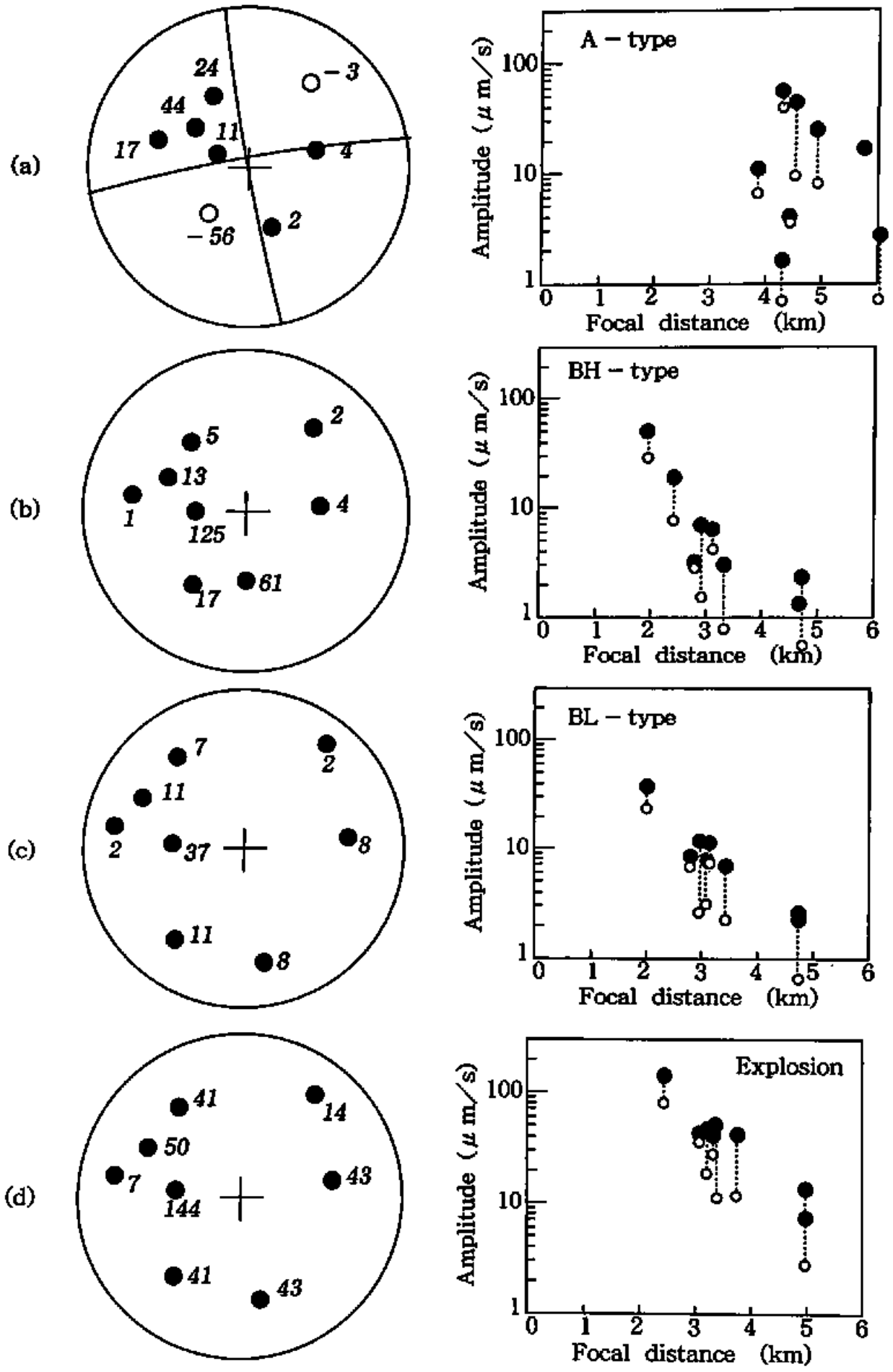


Fig. 8. Distribution of amplitudes of the first motions of P-waves. (Left): Amplitudes plotted on a map of an equal-area projection of the upper hemisphere of the focal sphere. Numerals denote amplitudes in μm/s. (Right): Plots of amplitudes against the focal distances to seismic stations. Open and solid circles represent the observed amplitudes and corrected ones for local site effects around the station, respectively. (a) A-type earthquake at 12:29, May 19, 1988, (b) BH-type earthquake at 12:08, September 4, 1987, (c) BL-type earthquake at 18:56, August 4, 1988 and (d) explosion earthquake at 00:59, April 15, 1988.

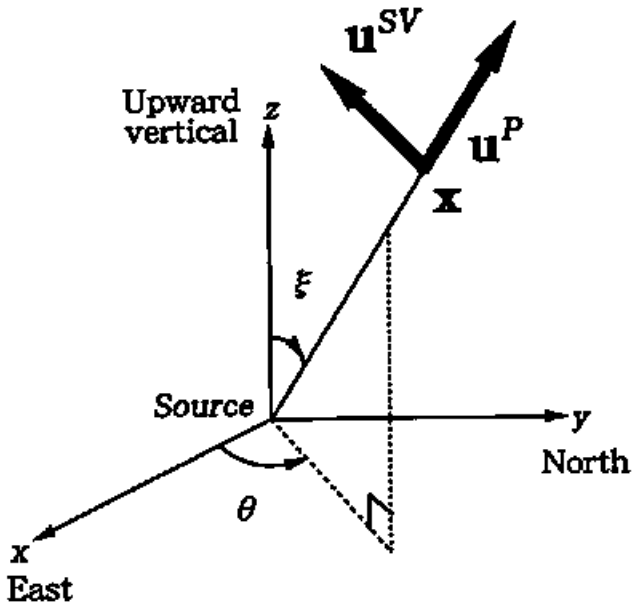


Fig. 9. A coordinates system employed in the present analysis.

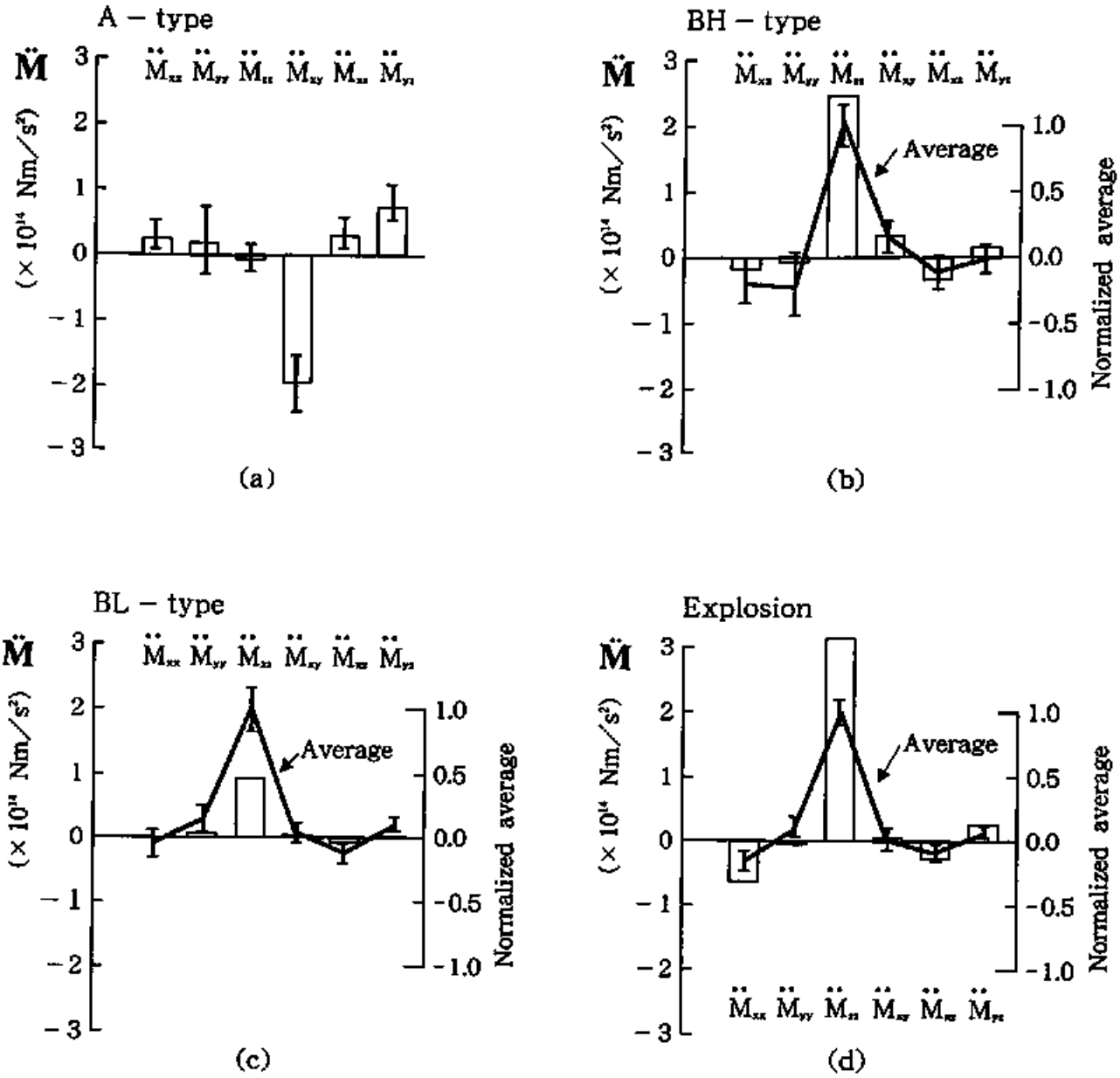


Fig. 10. Components of second derivative of moment tensor. (a) A-type earthquake at 12:29, May 19, 1988, (b) BH-type earthquake at 12:08, September 4, 1987, (c) BL-type earthquake at 18:56, August 4, 1988 and (d) explosion earthquake at 00:59, April 15, 1988. For BH-type, BL-type and explosion earthquakes, the averages of all components normalized by vertical vector dipole are shown by bold lines. Bars denote errors associated with the determination of the components.

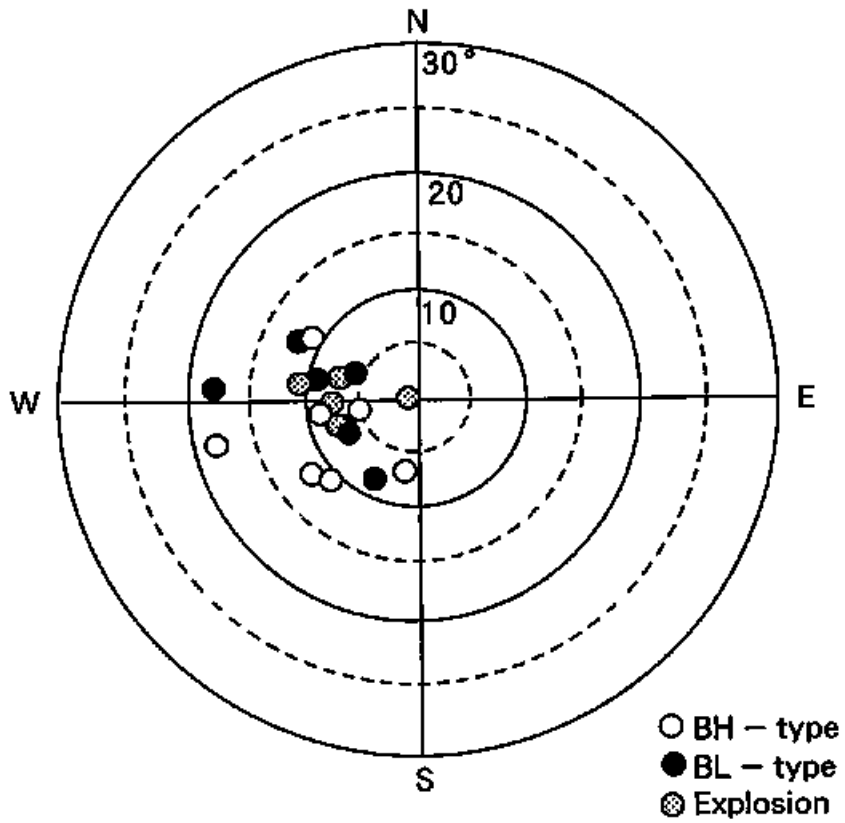


Fig. 11. Direction of dipoles. This diagram is an equal-area projection on the upper hemisphere of the focal sphere. Open, solid and shaded circles represent the azimuths and tilt angles of the dipoles of BH-type, BL-type and explosion earthquakes, respectively.

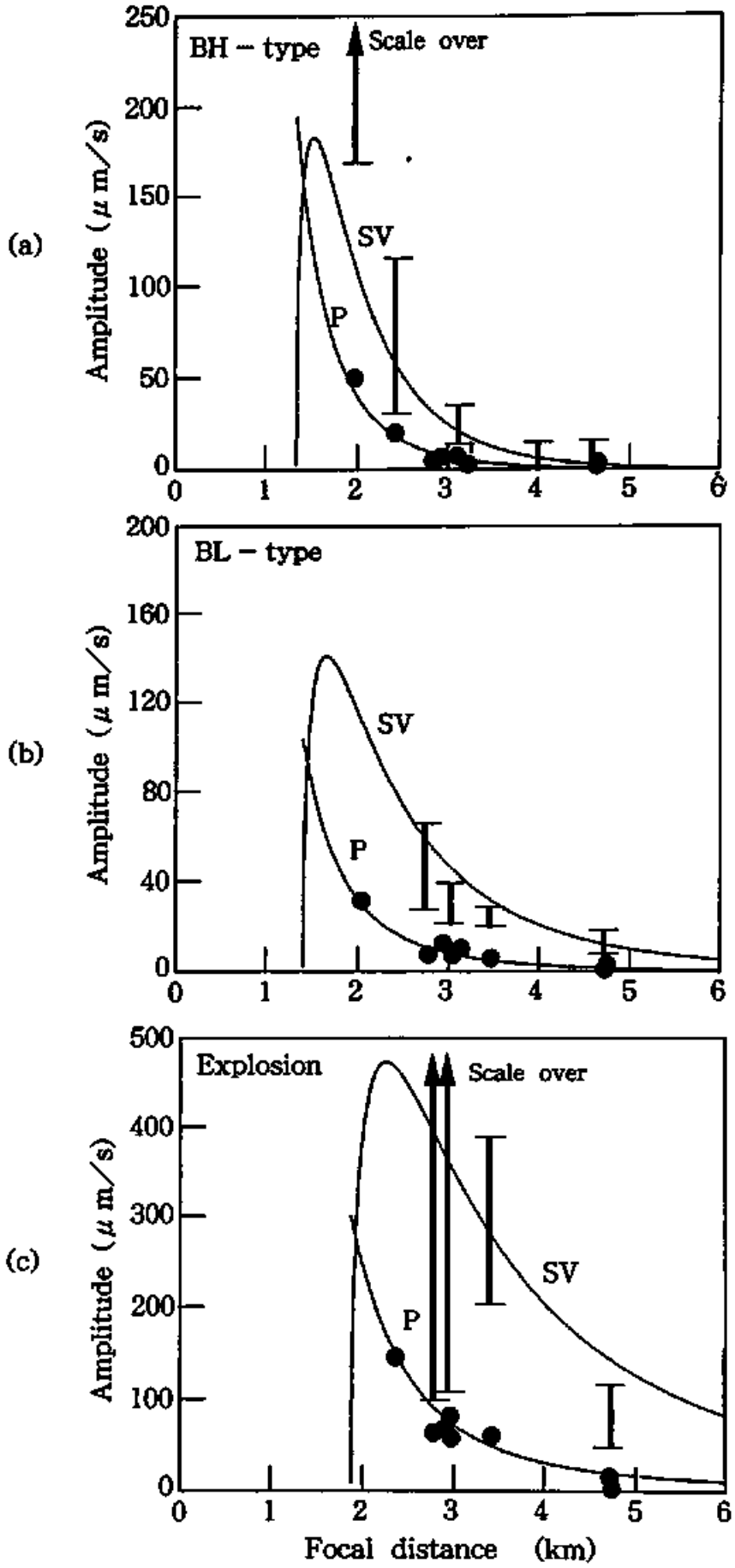


Fig. 12. Comparison between the theoretical and observed amplitudes of P- and SV-waves. Dots represent the observed amplitudes of the first motion of P-wave. Bars denote the range of observed amplitudes of SV-wave. The amplitudes are evaluated on the seismograms processed by applying a polarization filter. The note "Scale over" represents that velocity amplitudes exceed the range of recording. (a) BH-type earthquake at 19:43, September 4, 1987, (b) BL-type earthquake at 18:56, August 4, 1988 and (c) explosion earthquake at 00:59, April 15, 1988.

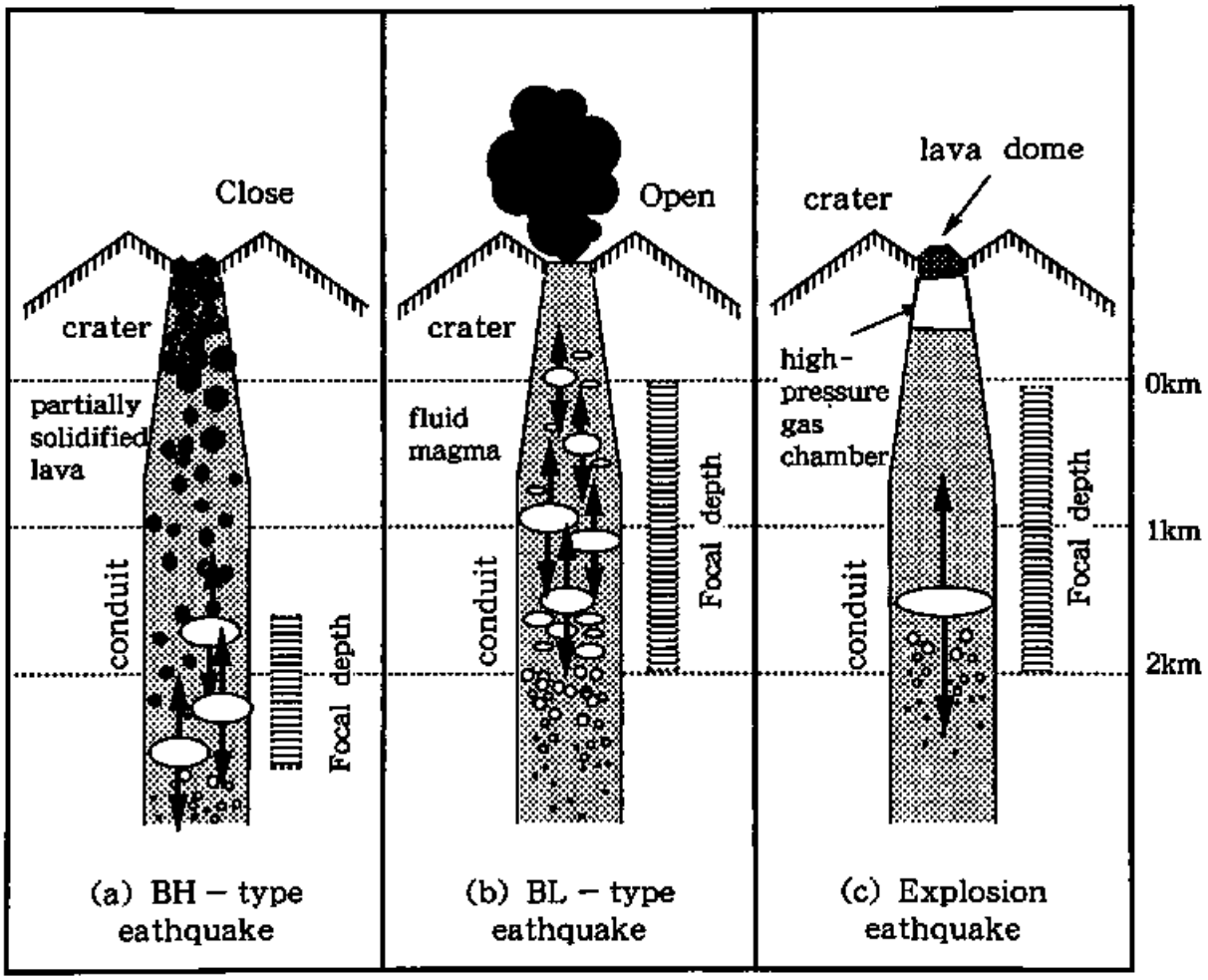


Fig. 13. Inferred states of the magma conduit during the swarms of BH-type and BL-type earthquakes and prior to the occurrence of explosion earthquakes. Hexagons and ellipses in the conduit represent solidified lavas and gas packets, respectively. Arrows indicate that gas pockets expand vertically along the conduit. Length of arrows represents the amplitude of the earthquakes schematically.